The Astrophysical Journal, 619:549–557, 2005 January 20

PREDICTING PLANETS IN KNOWN EXTRASOLAR PLANETARY SYSTEMS. II. TESTING FOR SATURN MASS PLANETS

Sean N. Raymond and Rory Barnes
Department of Astronomy, University of Washington, Seattle, WA 98195; raymond@astro.washington.edu, rory@astro.washington.edu
Received 2004 April 9; accepted 2004 September 28

ABSTRACT

Recent results have shown that many of the known extrasolar planetary systems contain regions that are stable for massless test particles. We examine the possibility that Saturn mass planets exist in these systems, just below the detection threshold, and predict likely orbital parameters for such unseen planets. We insert a Saturn mass planet into the regions stable for massless test particles and integrate the system for 100 million years. We conduct 200–600 of these experiments to test parameter space in 55 Cancri, HD 37124, HD 38529, and HD 74156. In 55 Cnc we find three maxima of the survival rate of Saturn mass planets, located in semimajor axis a and eccentricity e space at $(a, e) = (1.0$ AU, 0.02), (2.0 AU, 0.08), and (3.0 AU, 0.17). In HD 37124 the maximum lies at $a = 0.90-98$ AU, eccentricity $e \sim 0.05-0.15$. In HD 38529, only 5% of Saturn mass planets are unstable, and the region in which a Saturn mass planet could survive is very broad, centered on $0.5 < a < 0.6$, $e < 0.15$. In HD 74156 we find a broad maximum at $a = 0.9-1.4$ AU, $e \leq 0.15$. These orbital values are initial conditions, and not always the most likely values for detection. Several are located in the habitable zones of their parent stars and are of astrobiological interest. We suggest the possibility that companions may lie in these locations of parameter space, and encourage further observational investigation of these systems.

Subject headings: astrobiology — methods: *n*-body simulations — planets and satellites: formation

1. INTRODUCTION

There are currently 110 known extrasolar planets, including 10 systems containing two or more planets. These planets are known to be Jupiter-like both from their large masses, which range from $0.11M_J$ (HD 49674; Butler et al. 2003) to $17.5M_J$ (HD 202206; Udry et al. 2002), and from their sizes, measured in HD 209458b to be $1.27R_J$ (Charbonneau et al. 2000). The vast majority of these planets were discovered by the radial velocity technique, which is sensitive to roughly 3–10 m s^{-1} (Butler et al. 1996; Baranne et al. 1996).

All observed planetary systems must be dynamically stable for at least the age of their host star. Recent work by Barnes & Quinn (2004) suggests that a large fraction of systems are on the edge of stability: a small change in semimajor axis a or eccentricity e causes the system to become unstable. The "packed planetary systems" (PPS) hypothesis presented in Barnes & Raymond (2004, hereafter Paper I) predicts that all planetary systems are "on the edge." This leads to speculation that those systems that appear stable may harbor unseen planets that push them to the edge of stability. The PPS hypothesis suggests that if there exists a region in a planetary system in which the orbit of a massive planet is stable, then the region will contain a planet.

The first paper of this series (Paper I) used integrations of massless test particles to map the stability of regions in certain extrasolar planetary systems in (a, e)-space. Of the five systems examined, three (HD 37124, HD 38529, and 55 Cnc) were found to contain zones between the giant planets in which test particles were dynamically stable for 5–10 Myr. Stable regions have been found in a-space (assuming circular orbits) for υ And (Rivera & Lissauer 2000), GJ876 (Rivera & Lissauer 2001), and 55 Cnc (Rivera & Haghighipour 2003). This technique has been applied to numerous other extrasolar planetary systems not considered here (e.g., Jones et al. 2001; Jones & Sleep 2002; Noble et al. 2002).

In this work we test for the presence of unseen massive planets in four known extrasolar planetary systems: HD 37124 (Butler et al. 2003), HD 38529 (Fischer et al. 2003a), 55 Cnc (Marcy et al. 2001), and HD 74156 (Naef et al. 2004). We choose Saturn mass planets because they lie roughly at the detection threshold for the current radial velocity surveys (Butler et al. 1996). The reflex velocity caused by a Saturn mass planet at 1 AU on a solar mass star is 8.5 m s^{-1}, and scales as $a^{-1/2}$. For comparison, the smallest amplitude reflex velocity of any detected planet is 11 m s^{-1} (HD 1641; Marcy et al. 2000). Although seven sub–Saturn mass planets have been discovered as of 2003 November (e.g., Fischer et al. 2003b), none has $a > 0.35$ AU.[1] We run a small number of additional simulations with more massive test planets to dynamically constrain the mass of an unseen companion.

Paper I found that no test particles survived in HD 74156 for longer than a few Myr. Dvorak et al. (2003) found orbits stable for test particles between 0.9 and 1.4 AU. We include HD 74156 in our sample and show that Saturn mass test planets are stable in this system in many cases.

Table 1 shows the orbital parameters for the four extrasolar planetary systems we investigate. Note that the best-fit orbital elements for some systems, especially HD 74156c, have changed many times. We therefore adopt elements as of a given date, with the knowledge that they may fluctuate. In § 2 we describe our initial conditions and numerical method. We present the results for each planetary system in § 3 and compare these with other work in § 4. We present our conclusions in § 5.

2. NUMERICAL METHOD

For each planetary system in Table 1, 200–600 values of a and e are selected at random from within the regions that are stable for test particles, shown in Table 2. In the case of HD 74156, which has no stable region, we drew values from the following region: $\Delta a = 0.5-1.5$ AU, $\Delta e = 0.0-0.2$. For each of these (a, e)-points we assign the new planet one Saturn mass,

[1] Data from http://www.exoplanets.org.

TABLE 1
Orbital Parameters of Selected Planetary Systems

System	Planet	M (M_J)	a (AU)	e	ϖ	T (JD)
HD 37124[a]	b	0.86	0.54	0.1	97.0	2,451,227
	c	1.01	2.95	0.4	265.0	2,451,828
HD 38529	b	0.78	0.129	0.29	87.7	2,450,005.8
	c	12.8	3.68	0.36	14.7	2,450,073.8
55 Cnc	b	0.84	0.115	0.02	99.0	2,450,001.479
	c	0.21	0.241	0.339	61.0	2,450,031.4
	d	4.05	5.9	0.16	201.0	2,452,785
HD 74156[b]	b	1.61	0.28	0.647	185.0	2,451,981.38
	c	8.21	3.82	0.354	272.0	2,451,012.0

[a] Best-fit values for HD 37124 from Butler et al. (2003). The current best fit for planet c is $a = 2.50$ AU, $e = 0.69$ (see http://www.exoplanets.org).
[b] Best-fit values for HD 74156 as of 2002 August 22. The current best fit for planet c is $a = 3.40$ AU, $e = 0.58$ (Naef et al. 2004).

an inclination of $0.^\circ1$, and a randomly chosen mean anomaly. The longitude of periastron is aligned with the most massive giant planet in the system. This assumption helps find more stable systems, since most of the known planetary systems with ratios of orbital periods less than 5:1 are found to be librating about a common longitude of periastron (Ji et al. 2003 and references therein).

The four- or five-body system is integrated for 100 Myr or until the system becomes unstable through a collision or an ejection. We employ the hybrid integrator in mercury (Chambers 1999), which uses a second-order mixed variable symplectic algorithm when objects are separated by more than 3 Hill radii, and a Bulirsch-Stoer method for closer encounters. The time step in each system was chosen in order to sample the smallest orbit 20 times each period. Our integrations conserved energy to one part in 10^5. Each simulation took 0–10 days to run on a desktop PC, depending on the system and the outcome of the simulation (some systems resulted in ejections or collisions within a few wall clock minutes).

3. RESULTS

We present the results for three systems that were shown in Paper I to contain stable zones for massless test particles for at least 5–10 Myr. In addition, we examine the system HD 74156, which did not contain such a stable zone. In Table 2, we present the initial conditions for the simulations of each system, including the parameter space sampled and the number of Saturn mass planet experiments. Table 3 summarizes our results.

3.1. *55 Cancri*

This system is interesting dynamically, since it is composed of an interior pair of planets in close to 3:1 mean motion resonance and a distant, separated companion. Paper I showed that there is a large region between the inner pair and the outer planet that is stable for test particles, at 0.7 AU $< a <$ 3.4 AU, with eccentricities up to 0.2. This stable region is bounded at its inner edge by the 1:5 resonance, with the inner planet at 0.72 AU, and at its outer edge by the 5:2 resonance, with the outer planet at 3.2 AU. Several mean motion resonances with the outer planet are located in the stable region, notably the 3:1 resonance at 2.84 AU, the 4:1 resonance at 2.34 AU, and the 5:1 resonance at 2.02 AU.

TABLE 2
Initial Conditions for Simulations

System	Δa (AU)	Δe	N (Saturn Mass Planets)
HD 37124	0.9–1.1	0.0–0.2	472
HD 38529	0.27–0.82	0.0–0.3	200
55 Cnc	0.7–3.2	0.0–0.2	512
HD 74156[a]	0.5–1.5	0.0–0.2	600

[a] Paper I found that no test particles in HD 74156 survived for longer than 1 Myr. In our simulations, however, we sample the given region of parameter space.

We integrated the orbits of Saturn mass planets in 512 locations within this zone, and 384 (75%) of these survived for 100 Myr. Figure 1 shows the initial distribution in (a, e)-space of our experiments, in which solid dots represent stable simulations and plus signs represent unstable ones. Figure 2 shows the data binned in both the a- and e-axes such that each bin contains roughly 25 points. The shade of each square represents the fraction of planets in that bin that survived, and has a Poisson error of 20%. Overplotted are contours of constant survival rate, also spaced by 20%, to show the underlying distribution and the locations of maxima. The system's habitable zone (HZ) is marked by the dashed lines, calculated by the boundaries at which the aphelion or perihelion exits the HZ.

We see three local maxima in Fig. 2: (1) a relatively narrow maximum at $a \sim 1.0$ AU, $e \sim 0.03$; (2) a broad maximum centered roughly at $a \sim 2.0$ AU, $e \sim 0.08$ but that extends to higher values of a; and (3) $a \sim 3$ AU, $e \sim 0.17$. Region 1 is of great astrobiological interest, since it lies in the HZ of its parent star. Region 3 is bordered by the 3:1 (2.84 AU) and 5:2 (3.2 AU) mean motion resonances with the outer planet. We see no clear trend of survival rate with mean anomaly near these resonances.

Figures 1 and 2 refer to the test planets' initial orbital parameters and do not incorporate orbital variations over the course of each simulation. Figure 3 shows the orbital parameter space occupied by six stable Saturn mass planets throughout a 100 Myr integration, labeled by their starting parameters (a [AU], e). Each point represents a single output of one simulation, during which coordinates are output every 10^5 yr. Each test planet's semimajor axis and eccentricity change through the course of the integration, although the changes in a are typically much smaller than those in e. In addition, the amplitude of the variations differs significantly for different simulations. The simulation beginning at $(a, e) = (2.82\ \text{AU}, 0.07)$ reached a maximum eccentricity of 0.67 and had a mean of 0.33 over the

TABLE 3
SIMULATION RESULTS

System	Stable Region (a, e)[a]	Survival Rate[b]	Detection Region (a, e)[c]
55 Cnc	(1.0 AU, 0.03)[d]	93%	(1.0 AU, 0.07)
	(2.0 AU, 0.08)	89%	(2.0 AU, 0.08)
	(3.0 AU, 0.17)[e]	96%	(3.1 AU, 0.12)
HD 37124	(0.92 AU, 0.12)[d,e]	81%	(0.91 AU, 0.11)
	(0.96 AU, 0.07)[d,e]	87%	(0.95 AU, 0.09)
	(1.03 AU, 0.12)[d]	84%	(1.03 AU, 0.08)
HD 38529	(0.3–0.8 AU, 0.0–0.15)[e]	100%	(0.7 AU, 0.07)
HD 74156	(1.0 AU, 0.02)[d]	83%	(1.10 AU, 0.10)
	(1.0 AU, 0.10)[d]	83%	(1.10 AU, 0.10)
	(1.2 AU, 0.13)[e]	86%	(1.45 AU, 0.12)

[a] Local maxima of the survival rate, i.e., the center of each bin from Figs. 2, 7, 10, and 14 in which the survival rate is a maximum. The exact location of the stable region is uncertain on the order of the bin size. Note that these are initial conditions.

[b] Survival rate for all simulations with initial conditions in the binned region in which the stable region is located. See Figs. 2, 7, 10, and 14.

[c] Most likely region in parameter space to detect this planet. See Figs. 4, 9, 11, and 15.

[d] Stable regions that lie in the HZ of their parent stars, as defined by Kasting et al. (1993) and listed in Menou & Tabachnik (2003).

[e] Regions in which the survival rate of a small number of Jupiter mass test planets was within 30% of the rate for Saturn mass planets. In these regions we cannot tightly constrain the mass of an additional companion.

100 Myr simulation. In contrast, the simulation beginning at (2.45 AU, 0.10) never reached an eccentricity of less than 0.05 or more than 0.12.

The most likely orbit in which to observe a planet around another star is not the "initial condition." Rather, it is the place in parameter space in which the planet spends the most time. Figure 3 shows that a Saturn mass planet in 55 Cnc can evolve through a large amount of (a, e)-space and that the quantity varies for different starting orbits.

Figure 4 shows the relative time spent across parameter space by stable Saturn mass planets from each bin in Figure 2 with a survival rate of 75% or higher (those within the Poisson error). The shade of gray represents the total number of outputs from any simulation that fall in that bin, normalized to the maximum value. Contours are spaced by 20% in relative time, and each bin has been corrected for the uneven initial distribution of points. The relative time spent in each (a, e)-bin incorporates differences in survival rate and in the amplitude of secular a and e variations, and is a combination of all stable Saturn mass planets that spent time in that region. A maximum in relative time gives the orbital parameters at which an additional planet is most likely to be discovered in 55 Cnc.

It is interesting to compare the locations of maxima in Figures 2 and 4. Those in Figure 2 represent initial conditions most likely to be stable, while those in Figure 4 are regions in which stable test planets spend the most time. Maximum 1 from Figure 2 at $a \sim 1.0$ AU, $e \sim 0.03$ (as above) has been smeared out in Figure 4 and is located at higher eccentricities, between roughly 0.04 and 0.10. This smearing is due to the large eccentricity variations of Saturn mass planets in that region (seen in Fig. 3). Maxima 2 ($a \sim 2.0$ AU, $e \sim 0.08$) and 3 ($a \sim 2.0$ AU, $e \sim 0.08$) from Figure 2 are seen in Figure 4 in approximately the same locations, as well as two other maxima at $(a, e) \simeq (1.6$ AU, 0.07) and (2.6 AU, 0.09). In these locations the amplitude of

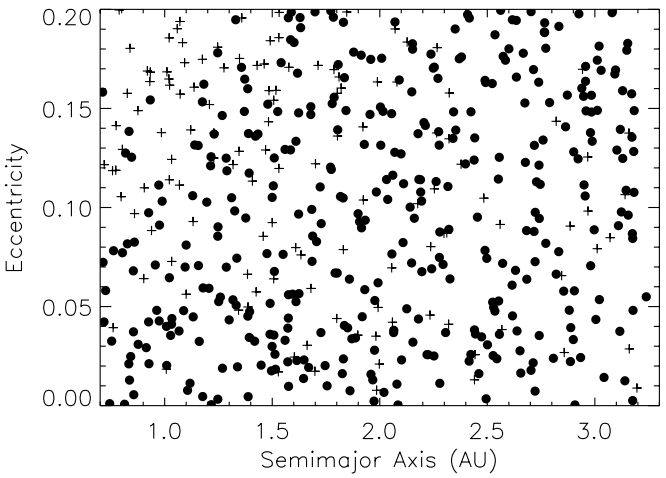

FIG. 1.—Initial distribution in (a, e)-space of 512 Saturn mass planets in 55 Cnc. Dots represent systems that were stable for 100 Myr and plus signs represent unstable simulations.

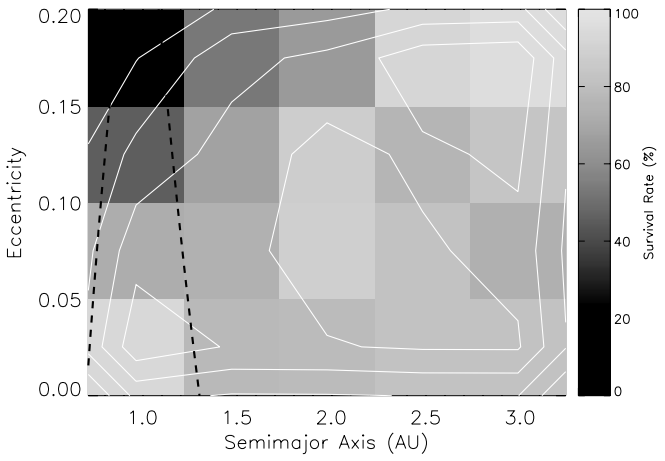

FIG. 2.—Data from 512 simulations of Saturn mass planets in 55 Cnc, binned on the a- and e-axes. The shade of each bin represents the fraction of planets in that bin that survived for 100 Myr, with Poisson errors of roughly 20%. Contours of constant survival rate are overplotted to bring out structure, spaced by 20%. The black dashed lines indicate the boundaries of the system's HZ. Note the maxima at $(a, e) \simeq (1.03$ AU, 0.03), (2.0 AU, 0.08), and (3.0 AU, 0.17).

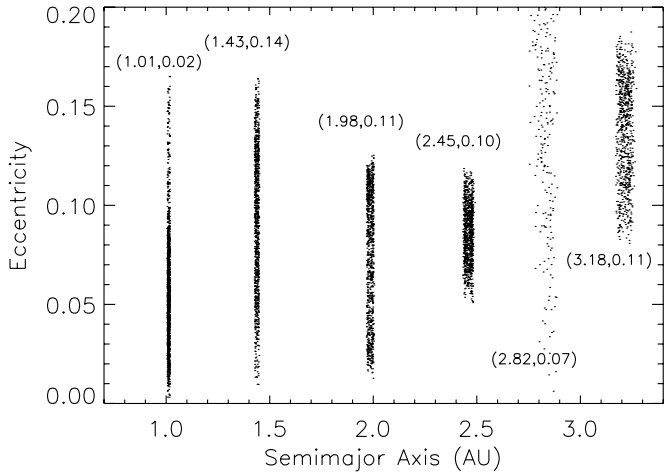

FIG. 3.—Orbital parameter space occupied by six Saturn mass planets in 55 Cnc, each of which was stable for 100 Myr. Each set of points is labeled by its starting orbital elements (a [AU], e). Each configuration is sampled every 10^5 yr.

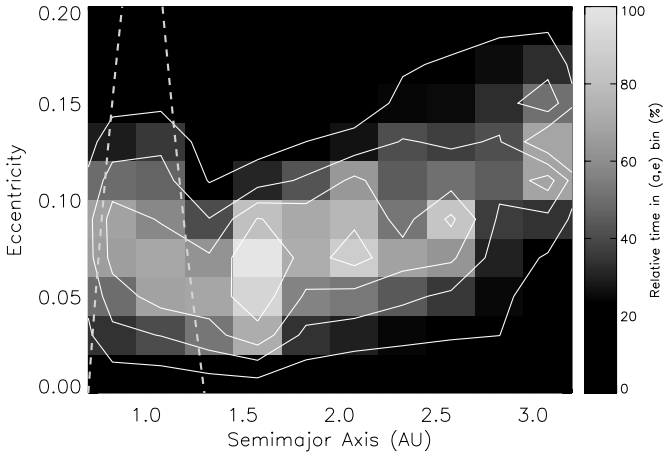

FIG. 4.—Time-averaged location in the parameter space of 55 Cnc for all stable simulations for each bin in Fig. 2 with a survival rate of 75% or higher. As in Fig. 3, each simulation comprises 1000 points (one output every 10^5 yr). Each bin is shaded according to the total number of points from all simulations falling in the region, and is corrected for the uneven initial distribution of simulations and scaled to the maximum value. A maximum in relative time corresponds to a location in (a, e)-space in which an additional companion is more likely to be detected.

eccentricity variations is small and the survival rate quite high, creating peaks in the relative time spent by test planets. There are other regions in Figure 4, such as $(a, e) \simeq (1.6\ \mathrm{AU}, 0.07)$, in which the time spent by test planets is a maximum. Although the survival rate of test planets with initial conditions in these regions was not a maximum, stable test planets spend a lot of time in these regions.

To test the sensitivity of these results to the mass of the test planet, we ran a small number of additional simulations including $1M_J$ and $10M_J$ planets. The reflex velocity of a star with such a planet would be large enough to surely have been detected. These simulations therefore indicate whether we can constrain the mass of a possible additional planet. These more massive test planets were placed in regions that were largely stable for Saturn mass planets (maxima 1, 2, and 3 from Fig. 2) and integrated for 100 Myr.

None of the $10M_J$ planets were stable. Three of 10 $1M_J$ planets placed in maximum 1 survived for 100 Myr, 10 of 20 survived in maximum 2, and seven of 10 survived in maximum 3. Table 3 shows that the survival rates of Saturn mass planets in the three maxima are 93% (maximum 1), 89% (maximum 2), and 96% (maximum 3), all of which are higher than those for $1M_J$ planets. This rate is significantly (2 σ or more) higher than that for $1M_J$ planets in maxima 1 and 2, but only slightly higher for maximum 3. Lower mass test planets are dynamically more stable in maxima 1 and 2 than more massive ones, so these regions are more likely to harbor lower mass planets, which fall roughly at or below current detection limits. We can therefore place a dynamical constraint on the mass of an unseen companion in maxima 1 and 2, in addition to the observational constraints. In maximum 3, however, we cannot.

3.2. *HD 37124*

This system has an interesting resonant structure. The ratio of the periods of the two known giant planets is 12.7, making it by far the most compact of our candidate systems. Three mean-motion resonances with the inner planet lie near the sampled region of parameter space—the 2:1 (0.86 AU), 3:1 (1.12 AU), and 5:2 (0.995 AU) resonances. The 5:2 resonance bisects the sampled region and has important consequences for the survival rate of test planets, as shown below.

Paper I showed that test particles are stable in HD 37124 for semimajor axes between 0.9 and 1.1 AU, with eccentricities between 0 and 0.25. We integrated the orbits of 472 Saturn mass planets in this system, 290 (61%) of which survived for 100 Myr.

In the absence of a test planet, the longitudes of periastron of the inner and outer giant planet librate about each other with an amplitude of roughly 31° and a precession period of 171 kyr. With the insertion of a Saturn mass test planet, we find evidence for secular resonances in various configurations of test planets. Figure 5 shows the time evolution of the longitudes of periastron of each planet in two stable cases. The initial orbital elements for the test planet in these systems are $(a, e) = (0.90\ \mathrm{AU}, 0.11)$ (*top*) and $(a, e) = (1.01\ \mathrm{AU}, 0.08)$ (*bottom*). The top panel shows a system in which the Saturn mass test planet is in a strong secular resonance with the inner giant planet, since the orientations of the two planets' orbits are tracking each other with time. The bottom panel shows a case in which the test planet's longitude of periastron (ϖ) is librating about that of the outer giant planet. At the same time, the test planet's orbit tracks that of the inner giant planet for over half of its precession cycle of ~7.5 kyr (e.g., 3500–7500 yr). An additional 1.5 kyr oscillation is superposed on the evolution of the test planet. The secular dynamics of the test planet in this case are affected by both giant planets in a complex way, yet the system is stable. Fourier transforms of the variables $h = e\cos(\varpi)$ and $k = e\sin(\varpi)$ show that the system is not chaotic. We expect systems in secular resonance to be stable because of the avoidance of close approaches between planets. Note in Figure 5 that the precession rates of both the inner and outer giant planets are different in the top and bottom panels, owing to the different locations of the test planet.

Figure 6 shows the survival rate of Saturn mass planets as a function of initial semimajor axis, including Poisson error bars. Note the strong decline in survival rate at the 2:5 mean motion resonance with the inner planet (located at 0.995 AU) and the peaks in survival rate immediately interior and exterior. There is a smaller peak at $a \simeq 0.90$ AU. We saw no strong dependence of the survival rate on mean anomaly in the resonance.

Figure 7 shows the survival rate binned in both initial semimajor axis and eccentricity, as in Figure 2. The outer edge of the system's HZ is marked by the black dashed line. Three local maxima are evident in the figure: (1) $a \sim 0.92$ AU, $e \sim 0.12$; (2) $a \sim 1.02$ AU, $e \sim 0.1$; and (3) the absolute maximum at

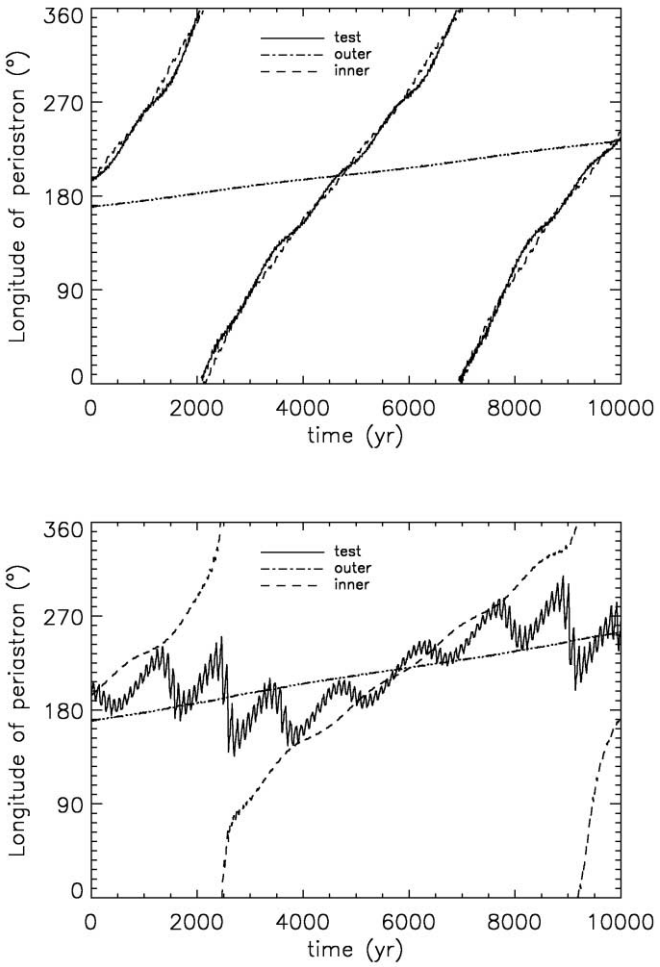

FIG. 5.—Evolution of the orientation of orbits (measured by the longitude of periastron) for two test systems of HD 37124. The initial orbital elements of the Saturn mass test planets are $(a, e) = (0.90\ \mathrm{AU}, 0.11)$ (*top*) and $(a, e) = (1.01\ \mathrm{AU}, 0.08)$ (*bottom*). Both systems were stable for 100 Myr and were sampled every year.

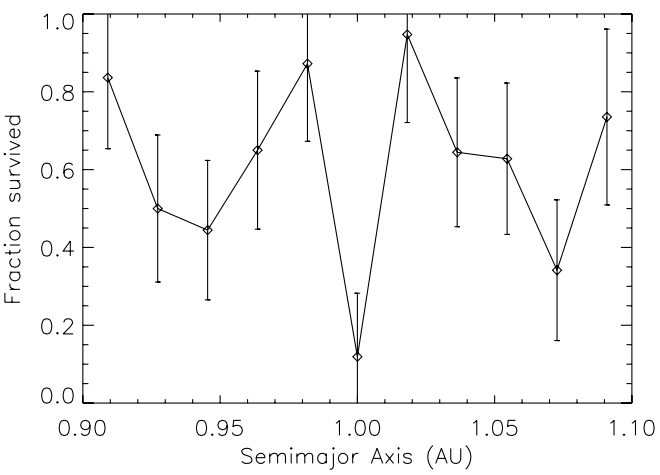

FIG. 6.—Survival rate of Saturn mass planets in HD 37124 as a function of initial semimajor axis, with Poisson error bars. Note the strong instability at the 2:5 mean motion resonance at 0.995 AU and the stable regions immediately interior and exterior.

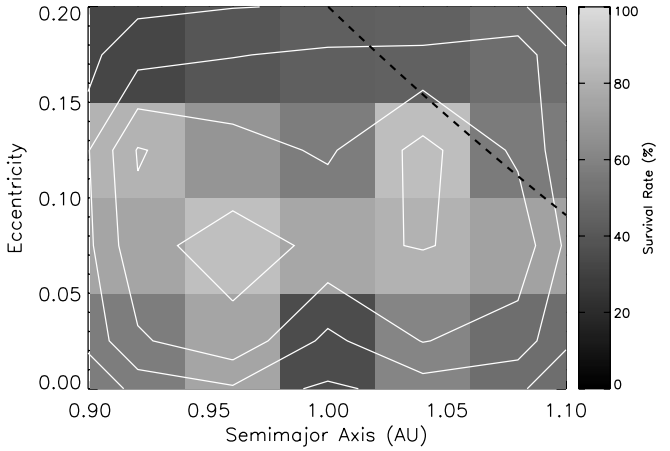

FIG. 7.—Binned survival rates for the initial conditions of 472 simulations in HD 37124, formatted as in Fig. 2. The black dashed line is the outer edge of the system's HZ. Note the three local maxima, including one on either side of the 2:5 resonance at 0.995 AU.

$a \sim 0.98$ AU, $e \sim 0.07$. Each of these maxima is located in the HZ of the system, although maximum 2 is at the outer edge.

Figure 8 shows the position in (a, e)-space of all stable test planets by small black dots, output at 10^5 yr intervals for the entirety of their 100 Myr integrations. The gray circles show the positions of all unstable simulations immediately before they became unstable. The 2:5 resonance with the outer planet is clearly unstable, as are certain other regions, some of which correspond to higher order mean motion resonances. There remain large areas in which no unstable systems reside, which correspond closely to the three maxima seen in Figure 7.

Figure 9 shows the time-integrated output of all stable simulations from bins in Figure 7 with survival rates of 70% or higher, formatted as in Figure 4. The dashed line represents the outer boundary of HD 37124's HZ. All three maxima from Figure 7 are apparent, with maximum 2 at 0.95 AU being the most prominent because of the interplay between the survival rate and amplitude of eccentricity variations.

We ran an additional 30 simulations with $1M_J$ test planets and 10 with $10M_J$ planets, initially placed in maxima 1, 2, and 3.

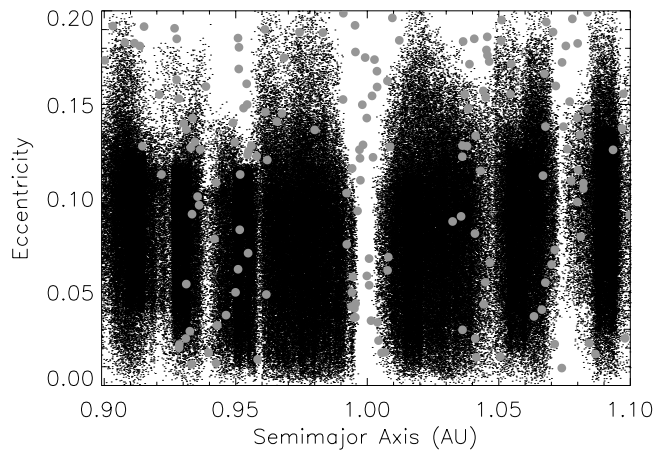

FIG. 8.—Regions in (a, e)-space occupied by stable Saturn mass planets in HD 37124. Each small black dot is a single data point from one simulation, output every 10^5 yr. The large gray dots indicate the location of unstable test planets immediately before disruption. Note the highly unstable nature of the 2:5 mean motion resonance at 0.995 AU, and the islands of stability associated with the three maxima from Fig. 7.

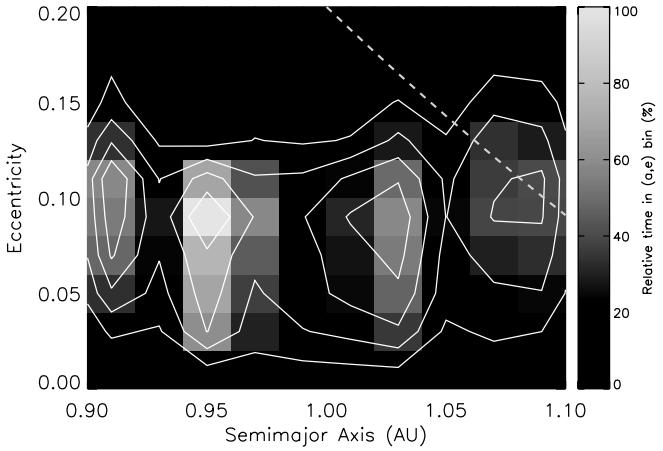

FIG. 9.—Relative time spent by stable Saturn mass planets in HD 37124 in (a, e)-space, formatted as in Fig. 4. All stable simulations in bins from Fig. 7 with survival rates of 70% or higher are included.

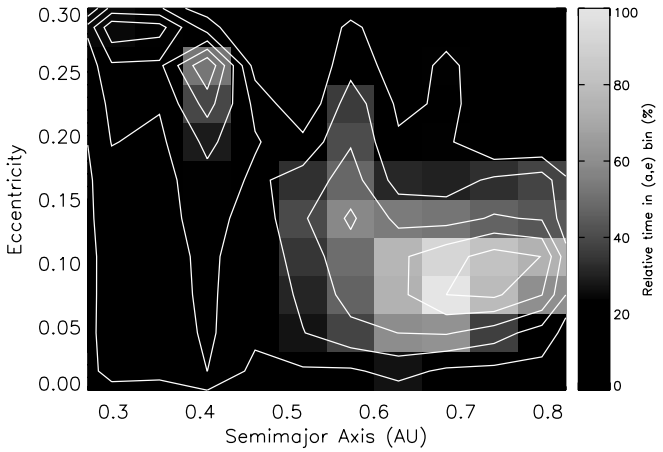

FIG. 11.—Relative time spent by stable simulations of HD 38529 in (a, e)-space, formatted as in Fig. 4. Only simulations at low-a and high-e (i.e., the four bins in the top left of Fig. 10) have been excluded.

None of the $10M_J$ planets survived. Six of 10 $1M_J$ planets survived in maximum 1, eight of 10 in maximum 2, and four of 10 in maximum 3. The survival rate of Saturn mass planets is between 81% and 89% for each maximum (see Table 3). In the case of maximum 2, the survival rate of Jupiter and Saturn mass planets is comparable, so we cannot dynamically constrain the mass of an unseen companion. For maxima 1 and 3 the survival rate is significantly lower for $1M_J$ planets, and we therefore suggest that, even in the absence of the observational constraints, these regions are more likely to harbor lower mass planets that fall close to the current observational limits.

3.3. *HD 38529*

The resonant structure of HD 38529 is quite different from that of HD 37124, since the separation between the two known planets is much larger. The stable region for test particles lies between 0.27 and 0.82 AU, with eccentricities up to 0.3. The inner edge is cut off by the 1:3 resonance with the inner planet. We see no evidence of secular resonances playing a significant role in the dynamics.

We integrated the orbits of 200 Saturn mass planets in this system, of which 191 (95.5%) survived for 100 Myr. Figure 10 shows the data binned in initial orbital elements and overplotted with contours as in Figure 7. The only unstable regions in this system lie at small semimajor axes and high eccentricities. The vast majority of the zone that is stable for massless test particles is also stable for Saturn mass planets.

Figure 11 shows the relative time spent in different regions of (a, e)-space by stable test planets from all bins in Figure 7 except those at low-a and high-e, formatted as in Figures 4 and 9. A strong maximum appears at $a \sim 0.7$, $e \sim 0.06-0.12$. As seen in previously discussed systems, this is due to the relatively small amplitude fluctuations in eccentricity experienced by stable test planets in this region.

Twenty additional simulations were performed, 10 with $1M_J$ planets and 10 with $10M_J$ planets. All of these were initially placed between 0.5 and 0.6 AU, with $e < 0.1$, and all were stable for 100 Myr. Consequently, we can put no dynamical upper bounds on the mass of an unseen companion in this region.

3.4. *HD 74156*

Paper I found that no test particles survived in this system for longer than 1 Myr. The region in which they survived the longest was for a between 0.5 and 1.5 AU at relatively low eccentricities. As discussed below, we find that a significant number of Saturn mass test planets survive in this system for 100 Myr. The reason for this appears to be a change in the

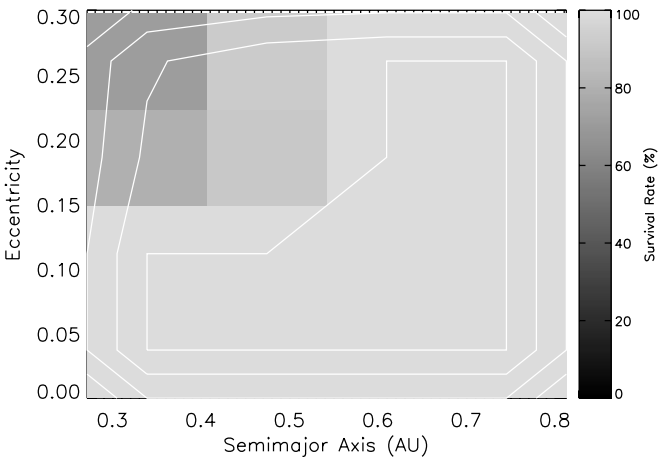

FIG. 10.—Binned data from the initial conditions of 200 simulations of Saturn mass planets in HD 38529 with contours of constant survival rate overplotted, as in Fig. 7. Contours of constant survival rate are spaced by 25%. The only unstable systems lie at low-a and high-e.

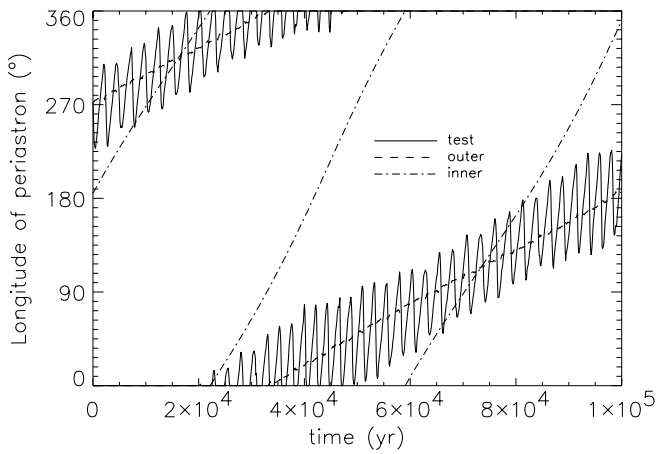

FIG. 12.—Evolution of the orientation of orbits (measured by the longitude of periastron) for one simulation of HD 74156, including a stable Saturn mass test planet. The initial orbital elements for the test planet are $(a, e) = (1.35\ \mathrm{AU}, 0.05)$.

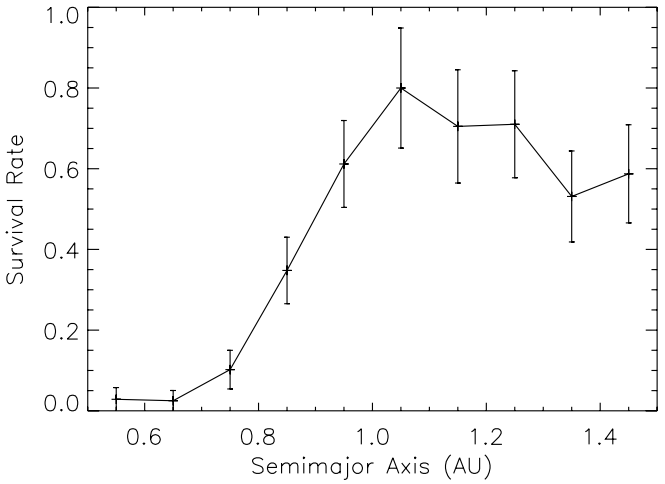

FIG. 13.—Survival rate of Saturn mass planets in HD 74156 as a function of initial semimajor axis, with statistical error bars. Note the strong increase toward 1 AU and the plateau between 1.0 and 1.4 AU.

secular dynamics of the system. A new frequency is introduced by the presence of the test planet. The outer giant planet and test planet librate about apsidal alignment at this new frequency in a stable fashion. Figure 12 shows one example, in which the test planet is librating about perfect alignment with the outer giant planet. The system was stable for 100 Myr.

The 1:5 mean motion resonance (with the inner planet) is at 0.82 AU and the 5:1 resonance (with the outer planet) at 1.3 AU is located at the outskirts of the region we investigate. Therefore, only very high order mean motion resonances are found in the center.

We performed 600 integrations of Saturn mass planets in this system with a in the above-mentioned region and e between 0 and 0.2. Of these 600 Saturn mass planets, 296 (49%) survived for 100 Myr. Figure 13 shows a strong trend in the survival rate of planets as a function of initial semimajor axis. The fraction of systems that are stable for 100 Myr increases sharply between 0.8 and 1.0 AU, then flattens off and decreases slightly past 1.2 AU. The stable zones found in Figure 14 lie at the peak of the curve.

Figure 14 shows the survival rate of planets as a function of their initial orbital parameters. We see three small islands

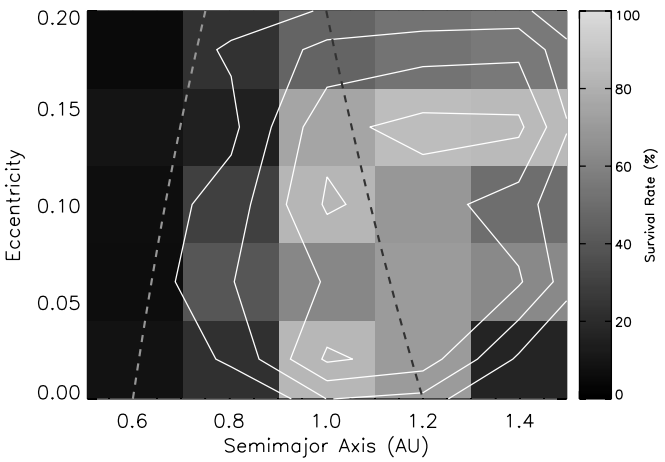

FIG. 14.—Binned data from the initial conditions of 600 simulations of Saturn mass planets in HD 74156, formatted as in Fig. 2, with contours of constant survival rate spaced by 20%. The dashed lines indicate the boundaries of the system's HZ. The absolute maximum is located at $(a, e) \simeq (1.0$ AU, 0.02), and two local maxima are at $(a, e) \simeq (1.0$ AU, 0.10) and (1.2 AU, 0.13).

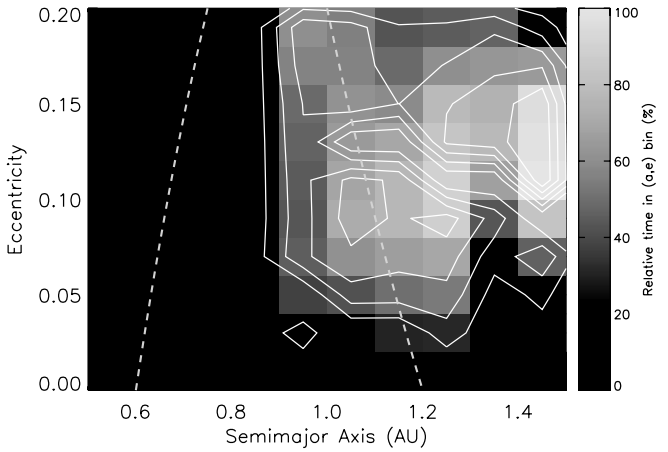

FIG. 15.—Relative time spent in (a, e)-space by all stable simulations of HD 74156 from bins in Fig. 14 with survival rates greater than 68%, formatted as in Fig. 4.

of stability at (1) $(a, e) \simeq (1.0$ AU, 0.02), (2) $(a, e) \simeq (1.0$ AU, 0.1), and (3) $(a, e) \simeq (1.2$ AU, 0.13). These three islands lie at a slightly higher survival rate than the surrounding, larger region of stability between 0.9 and 1.2 AU with $e \leq 0.15$, in which the survival rate is 75%. Two of these islands lie in the HZ.

Figure 15 shows the relative time spent across orbital parameter space by all stable simulations from bins in Figure 13 with survival rates higher than 68%. All three maxima from Figure 14 combine to form a large plateau in which an unseen companion is most likely to be detected, at 1.0 AU $< a <$ 1.4 AU, $0.05 < e < 0.18$. The peak is located at $a \sim 1.4$ AU, $e \sim 0.14$, again because of a combination of high survival rate and low-amplitude eccentricity variations.

We ran 40 additional simulations in HD 74156 including more massive test planets: 30 with $1M_{\rm J}$ planets and 10 with $10M_{\rm J}$ planets. Only one of the $10M_{\rm J}$ planets was stable. Four of 10 $1M_{\rm J}$ planets were stable in maximum 1, four of 10 in maximum 2, and eight of 10 in maximum 3. The survival rates for Saturn mass test planets of the three maxima are slightly greater than 80% (see Table 3). We therefore dynamically constrain to lower values the mass of a potential unseen companion in maxima 1 and 2, but not in maximum 3.

4. DISCUSSION

Menou & Tabachnik (2003, hereafter MT03) investigated the possibility of Earth-sized planets residing in the HZs of known extrasolar planetary systems. The location of the HZ is a function of the luminosity (and therefore mass) of the host star, as well as the atmospheric composition of the planet (Kasting et al. 1993). For each system MT03 integrated the orbits of 100 massless test particles in the HZ for 10^6 yr. They considered all four of our systems. The HZs for each system are: HD 37124, 0.6–1.2 AU; HD 38529, 1.4–3 AU; HD 74156, 0.6–1.2 AU; and 55 Cnc, 0.7–1.3 AU. MT03 found no surviving planets in the HZ of HD 37124. Their stability criterion requires a particle to remain in the HZ at all times, limiting its eccentricity such that the particle's aphelion and perihelion remain in the HZ. Paper I used over 500 test particles to systematically map out the region in HD 37124 that is stable for test particles, finding it to be centered at 1 AU. The eccentricities in this stable region are small enough to keep test particles in the HZ of the system throughout their orbits. In addition, we find three local maxima of the survival rate of Saturn mass planets in this system, all of whose orbits remain in the HZ. Note that the orbital

elements for the two planets around HD 37124 have recently been revised.[2] In particular, the best-fit orbit of the outer planet is now $a = 2.50$ AU, $e = 0.69$, greatly reducing the possibility of stable regions between planets b and c.

For HD 38529 our results are consistent with MT03, since the stable region from Paper I lies well outside the HZ, and the region we investigated with Saturn mass planets does not overlap the HZ. In the case of 55 Cnc our results are again consistent with MT03, who find that a significant fraction of low-inclination test particles survive at 1.0 AU, with eccentricities centered on 0.09. The stable region for 55 Cnc from Paper I encompasses the HZ entirely for eccentricities below 0.25. In addition, Table 3 shows a maximum in the survival rate of Saturn mass planets at $(a, e) \simeq (1.0\ \mathrm{AU}, 0.03)$, very close to the value from MT03. The results of MT03 for HD 74156 are consistent with Paper I, but we have found two regions in the HZ that are stable for Saturn mass planets in 83% of cases. This may be due to the fact that the orbital elements used by MT03 are different from those we have used here. In particular, the semimajor axis of the outer planet used here is 0.35 AU larger (3.82 vs. 3.47 AU), increasing the separation of the two giant planets and therefore possibly causing the region in between to become more stable for an additional companion. Note that the current value for HD 74156c is 3.40 AU (Naef et al. 2004).

Dvorak et al. (2003) investigated the possibility of an unseen planet in HD 74156, using both test particles and massive ones. They find a broad, relatively stable region for test particles between 0.9 and 1.4 AU, with the most stable location being at $a = 1.25$ AU and $e < 0.2$. This is a region in which Paper I found no stable test particle orbits. Figure 13 shows a plateau in survivability between 1.0 and 1.25 AU. Dvorak et al. (2003) found no trend in the results of their simulations of massive planets, and concluded that the presence of an unseen companion in the system was unlikely. Further observations will shed light on this issue, although the 75% survival rate of Saturn mass planets for the entire region with $0.9\ \mathrm{AU} < a < 1.2\ \mathrm{AU}$, $e \leq 0.15$ suggests that this is a real possibility. Note again that the best-fit orbit of the outer planet in this system has recently been revised to $a = 3.40$ AU, $e = 0.58$ (Naef et al. 2004). The closer proximity and higher eccentricity of this planet strongly affect the dynamics between the two known plants. Both Dvorak et al. (2003) and Paper I assume the orbital elements from Table 1 in their calculations.

5. CONCLUSIONS

We have found specific locations in four known extrasolar planetary systems in which Saturn mass planets could exist on stable orbits. Such a planet would lie just below the detection threshold of current radial velocity surveys, but may be detected in the near future. Table 3 summarizes our results, detailing the location in (a,e)-space of each maximum in the survival rate for each of our four candidate systems. Because of orbital variations, the most likely place to detect planets is often not at the "initial conditions," as shown in Figures 4, 9, 11, and 15.

Does the presence of a stable region imply the presence of a planet? Must all systems contain as many planets as possible? Laskar (1996) speculated that "a planetary system will always be in this state of marginal stability, as a result of its gravitational interactions." The "packed planetary systems" (PPS) hypothesis, presented in Paper I (see also Barnes & Quinn 2004), extends this idea by suggesting that all systems contain as many planets as they can dynamically support without self-disrupting. All systems may be on the edge of stability, but observational constraints prevent the detection of smaller or more distant bodies that push apparently stable systems to this edge.

Some of the maxima in Table 3 are stable for Saturn mass planets but not for Jupiter mass planets. In such a case a planet is more likely to exist below the detection threshold, simply because the system is more stable. Certain maxima are as stable for Jupiter mass planets as for Saturn mass planets. In these cases we cannot dynamically constrain the mass of a possible unseen companion. The PPS hypothesis suggests that every stable region in a planetary system is occupied, although the body need not have the maximum possible stable mass. This is illustrated in our simulations of HD 38529, which contains a region that is stable for Saturn mass, $1M_{\mathrm{J}}$, and even $10M_{\mathrm{J}}$ test planets, but observations constrain the mass of any unseen planet to be roughly a Saturn mass or less.

The formation scenario of a planet of any size in between two gas giant planets is of great interest. In the solar system, no stable region exists between the orbits of the gas giants. The detailed formation scenario of a smaller giant planet between two others is unclear, be it through gravitational instability (e.g., Mayer et al. 2002) or core accretion (Pollack et al. 1996). Gas giant planets at small orbital radii may have formed farther out in the protoplanetary disk and migrated inward, which further complicates this formation scenario.

Certain stable regions in HD 37124, 55 Cnc, and HD 74156 are located in the HZs of their parent stars (see Table 3). The possible existence of potentially habitable, Earth-like planets in these regions is of great astrobiological interest. Raymond et al. (2004) show that terrestrial planets can form in the presence of close-in extrasolar giant planets, despite the giant planets having likely migrated through the terrestrial region. In the upcoming third paper of the "predicting planets" series (Raymond & Barnes 2004), we present results of simulations of terrestrial planet formation in between the known giant planets in the same four systems examined here.

We thank Tom Quinn and Andrew West for many helpful discussions, and Chance Reschke for his assistance in the completion of the simulations presented in this paper. This work was funded by grants from the NASA Astrobiology Institute, the NSF, and a NASA GSRP. These simulations were performed on computers donated by the University of Washington Student Technology Fund. These simulations were performed under CONDOR.[3]

[2] See http://www.exoplanets.org.

[3] CONDOR is publicly available at http://www.cs.wisc.edu/condor.

REFERENCES

Baranne, A., et al. 1996, A&AS, 119, 373
Barnes, R., & Quinn, T. 2004, ApJ, 611, 494
Barnes, R., & Raymond, S. N. 2004, ApJ, 617, 569 (Paper I)
Butler, R. P., Marcy, G. W., Vogt, S. S., Fischer, D. A., Henry, G. W., Laughlin, G., & Wright, J. T. 2003, ApJ, 582, 455
Butler, R. P., Marcy, G. W., Williams, E., McCarthy, C., Dosanjh, P., & Vogt, S. S. 1996, PASP, 108, 500
Chambers, J. E. 1999, MNRAS, 304, 793
Charbonneau, D., Brown, T. M., Latham, D. W., & Mayor, M. 2000, ApJ, 529, L45
Dvorak, R., Pilat-Lohinger, E., Funk, B., & Freistetter, F. 2003, A&A, 410, L13

Fischer, D. A., et al. 2003a, ApJ, 586, 1394
Fischer, D. A., Butler, R. P., Marcy, G. W., Vogt, S. S., & Henry, G. W. 2003b, ApJ, 590, 1081
Ji, J., Liu, L., Kinoshita, H., Zhou, J., Nakai, H., & Li, G. 2003, ApJ, 591, L57
Jones, B. W., & Sleep, P. N. 2002, A&A, 393, 1015
Jones, B. W., Sleep, P. N., & Chambers, J. E. 2001, A&A, 366, 254
Kasting, J. F., Whitmire, D. P., & Reynolds, R. T. 1993, Icarus, 101, 108
Laskar, J. 1996, Celest. Mech. Dyn. Astron., 64, 115
Marcy, G. W., Butler, R. P., & Vogt, S. S. 2000, ApJ, 536, L43
Marcy, G. W., et al. 2001, ApJ, 555, 418
Mayer, L., Wadsley, J., Quinn, T., & Stadel, J. 2002, Science, 298, 1756
Menou, K., & Tabachnik, S. 2003, ApJ, 583, 473 (MT03)
Naef, D., Mayor, M., Beuzit, J. L., Perrier, C., Queloz, D., Sivan, J. P., & Udry, S. 2004, A&A, 414, 351
Noble, M., Musielak, Z. E., & Cuntz, M. 2002, ApJ, 572, 1024
Pollack, J. B., Hubickyj, O., Bodenheimer, P., Lissauer, J. J., Podolak, M., & Greenzweig, Y. 1996, Icarus, 124, 62
Raymond, S. N., & Barnes, R. 2004, ApJ, submitted (astro-ph/0404212)
Raymond, S. N., Quinn, T., & Lunine, J. I. 2004, Icarus, submitted (astro-ph/0407620)
Rivera, E. J., & Haghighipour, N. 2003, in ASP Conf. Ser. 294, Scientific Frontiers in Research on Extrasolar Planets, ed. D. Deming & S. Seager (San Francisco: ASP), 205
Rivera, E. J., & Lissauer, J. L. 2000, ApJ, 530, 454
———. 2001, ApJ, 558, 392
Udry, S., Mayor, M., Naef, D., Pepe, F., Queloz, D., Santos, N. C., & Burnet, M. 2002, A&A, 390, 267